AGU PUBLICATIONS

JGR

Journal of Geophysical Research: Atmospheres

RESEARCH ARTICLE
10.1002/2016JD024814

Key Points:
- Biogeochemical and biogeophysical ecosystem-climate feedback are quantified and compared
- Northern terrestrial ecosystems will cause a net positive radiative forcing over this century
- CH_4-related biogeochemical effects play an important role in regulating ecosystem-climate feedback

Supporting Information:
- Figures S1 and S2

Correspondence to:
Q. Zhuang,
qzhuang@purdue.edu

Citation:
Zhu, X., and Q. Zhuang (2016), Relative importance between biogeochemical and biogeophysical effects in regulating terrestrial ecosystem-climate feedback in northern high latitudes, *J. Geophys. Res. Atmos.*, *121*, 5736–5748, doi:10.1002/2016JD024814.

Received 18 JAN 2016
Accepted 16 MAY 2016
Accepted article online 19 MAY 2016
Published online 31 MAY 2016

Relative importance between biogeochemical and biogeophysical effects in regulating terrestrial ecosystem-climate feedback in northern high latitudes

Xudong Zhu[1,2,3] and Qianlai Zhuang[3,4]

[1]Key Laboratory of the Coastal and Wetland Ecosystems, Ministry of Education, Xiamen University, Xiamen, China, [2]State Key Laboratory of Remote Sensing Science, Institute of Remote Sensing and Digital Earth, Chinese Academy of Sciences, Beijing, China, [3]Department of Earth, Atmospheric, and Planetary Sciences, Purdue University, West Lafayette, Indiana, USA, [4]Department of Agronomy, Purdue University, West Lafayette, Indiana, USA

Abstract Warming-induced changes in structures and functions of northern terrestrial ecosystems (NTEs), including their regulation on terrestrial biogeochemistry and surface energy balance, may exert positive or negative feedback to the climate system. However, the relative importance among these biogeochemical and biogeophysical feedback is not well understood. Here we use a terrestrial ecosystem model to quantify spatially explicit ecosystem-climate feedback over NTEs (north of 50°N) under four climate change scenarios from 2010 to 2100, including biogeochemical feedback from climate-induced changes in net CH_4 exchanges (NME) and net CO_2 exchanges (NCE) and biogeophysical feedback from changes in surface energy partitioning associated with snow cover and vegetation biomass dynamics. Our results indicate that (1) biogeochemical and biogeophysical feedback are attributed more to the changes in NME and snow cover dynamics, respectively; (2) net biogeophysical feedback is much larger than net biogeochemical feedback; (3) NTEs will cause a net positive radiative forcing of 0.04–0.26 W m^{-2} between 2010 and 2100. Our findings support the notion that NTEs will exert positive net climate feedback; however, our estimation of positive net biogeochemical feedback including NME- and NCE-induced effects is contrary to previous studies showing negative net biogeochemical feedback including NCE-induced effect only. This study highlights the importance of NME-induced biogeochemical effect in regulating ecosystem-climate feedback in NTEs and implies that previous studies without considering NME-induced effect might have underestimated the intensity of total terrestrial feedback to the climate system.

1. Introduction

The atmospheric concentrations of greenhouse gases (GHG), such as carbon dioxide (CO_2) and methane (CH_4), have all increased significantly since preindustrial times mainly due to fossil fuel emissions and land use change emissions [*Stocker et al.*, 2013]. Consequently, the Earth has experienced surface warming with a global increase of 0.85°C since 1880 and potentially another increase of 1.0–3.7°C at the end of this century [*Stocker et al.*, 2013]. Northern high latitudes have experienced a larger increase in surface air temperature in comparison with the global average increase [*Polyakov et al.*, 2002; *Euskirchen et al.*, 2007; *Comiso and Hall*, 2014]. This temperature increase has modified the structures and functions of northern terrestrial ecosystems (NTEs), including their biogeochemical and biogeophysical feedback to the climate system [*Field et al.*, 2007].

On the one hand, NTEs play an important role in the global GHG dynamics (biogeochemical feedback) with an estimated sink of atmospheric CO_2 and a source of atmospheric CH_4 under contemporary climate conditions [*McGuire et al.*, 2009; *Zhu et al.*, 2013a; *Zhuang et al.*, 2015]. Given that NTEs have undergone dramatic climate-induced environmental changes in recent decades including rising temperatures, permafrost thawing, and prolonged growing season [*Romanovsky et al.*, 2000; *Piao et al.*, 2007; *Pieter and Scott*, 2011], and that these changes are likely to be more dramatic in the future [*Stocker et al.*, 2013], NTEs are expected to continue to affect the climate system through an even larger biogeochemical feedback. On the other hand, the region's biogeophysical feedback to the climate system are also important since climate change will affect land surface energy budget by modifying biogeophysical properties including albedo, the roughness, and the partitioning pattern of sensible and latent heat fluxes [*Brovkin et al.*, 2006; *Bonfils et al.*, 2012].

For example, positive biogeophysical feedback due to reduced surface albedo from warming-induced snow cover retreat and greener vegetation in growing season has a large potential to amplify regional warming [*Chapin et al.*, 2005; *Euskirchen et al.*, 2007].

Biogeochemical and biogeophysical feedback of terrestrial ecosystems are linked processes, in which biogeophysical impacts are connected with biogeochemical impacts through their influence on terrestrial GHG and water cycles [*Bonan*, 2008; *Zhang et al.*, 2014]. To appropriately quantify terrestrial feedback to the atmosphere, both biogeochemical and biogeophysical impacts should be included. Many previous ecosystem-climate feedback studies explored either terrestrial biogeochemical [e.g., *Friedlingstein et al.*, 2006; *Qian et al.*, 2010; *McGuire et al.*, 2012] or biogeophysical [e.g., *Bala et al.*, 2006; *Betts et al.*, 2007] feedback to the atmosphere. Although there were quite some studies covering both feedback [e.g., *Betts*, 2000; *Claussen et al.*, 2001; *Bathiany et al.*, 2010], these studies examined feedback based on idealized land cover transitions through conducting large-scale afforestation or deforestation model experiments. Only a few studies explicitly considered and quantified both feedback from realistic and transient land surface dynamics [*Lohila et al.*, 2010; *Zhang et al.*, 2014]. Furthermore, previous studies only considered CO_2-related climate feedback without the contribution from CH_4 emissions, which might largely affect accurate quantification of biogeochemical feedback of NTEs given that the CH_4-related climate feedback in this region is of a same order of magnitude as CO_2-related feedback [*Zhu et al.*, 2013a].

To quantify terrestrial ecosystem-climate feedback, it would be ideal to apply Integrated Earth System Models, in which biogeochemical and biogeophysical feedback mechanisms are explicitly represented and land surface processes and climate dynamics are tightly coupled. However, this could be an extremely challenging task because of the complex nature of the expected two-way dynamic interactions between terrestrial ecosystems and the climate system, our limited understanding of underlying mechanisms for these dynamical interactions, and high computational cost of performing these types of model simulations. An important first step would be to assess the relative importance among different feedback mechanisms, based on uncoupled simulations using stand-alone land surface models, to increase our understanding of complex terrestrial feedback to the atmosphere. To this end, we applied a terrestrial ecosystem model to simulate terrestrial CO_2 and CH_4 cycles, snow cover, and vegetation biomass dynamics in NTEs under multiple future climate change scenarios, and then assessed the relative importance between biogeochemical and biogeophysical feedback arising from these climate-induced structural and functional changes of NTEs. Specifically, we investigated the following questions: (1) How will the climate-induced changes in land-atmospheric CO_2 and CH_4 exchanges affect terrestrial biogeochemical feedback? (2) How will the climate-induced changes in snow cover and vegetation biomass dynamics affect terrestrial biogeophysical feedback? (3) What is relative importance between biogeochemical and biogeophysical feedback? (4) Will NTEs exert a positive or negative net feedback to the climate system?

2. Methods

2.1. Overview

A process-based ecosystem model, the Terrestrial Ecosystems Model (TEM), was used to simulate spatially explicit ecosystem carbon and snow cover dynamics of NTEs in response to climate change over 2010–2100. The changes in simulated land-atmospheric CO_2 and CH_4 exchanges over the years were used to calculate terrestrial biogeochemical feedback, and the changes in simulated snow cover and vegetation biomass were used to calculate terrestrial biogeophysical feedback. To make biogeochemical and biogeophysical feedback comparable, the magnitude of feedback were consistently expressed as global-mean radiative forcing between 2010 and 2100.

2.2. Model and Data

TEM is a process-based terrestrial ecosystem model that simulates terrestrial carbon, water, and nutrient dynamics and their interactions in plants and soils [*Raich et al.*, 1991; *Zhuang et al.*, 2003, 2004; *McGuire et al.*, 2010; *Zhuang et al.*, 2010]. It contains several modules including soil thermal module (STM), hydrological module (HM), carbon and nitrogen dynamic module (CNDM), and methane dynamic module (MDM). These modules are closely coupled to simulate soil thermal and hydrological dynamics as well as biogeochemical processes in terrestrial ecosystems. The STM has been developed to simulate soil thermal dynamics in

Table 1. Annual Changing Rates of Global Mean Atmospheric CO_2 Concentrations and Regional Mean Climate Conditions Over Northern Terrestrial Ecosystems (North of 50°N) From 2011 to 2100, Under Four Climate Change Scenarios[a]

	RCP2.6	RCP4.5	RCP6.0	RCP8.5
CO_2 concentration (ppm yr^{-1})	0.20 (0.15)	1.81 (0.94)	3.21 (0.98)	6.10 (0.97)
Air temperature(°C yr^{-1})	0.02 (0.47)	0.04 (0.87)	0.05 (0.95)	0.08 (0.97)
Precipitation(mm yr^{-1})	0.35 (0.33)	0.54 (0.56)	0.82 (0.74)	1.09 (0.89)
Incoming shortwave radiation (W m^{-2} yr^{-1})	0.02 (0.37)	0.01 (0.16)	−0.00 (0.00)*	−0.02 (0.32)
Relative humidity(% yr^{-1})	−0.01 (0.31)	−0.02 (0.79)	−0.03 (0.86)	−0.04 (0.93)

[a]The changing rates are determined as the slopes from least squares linear regressions (corresponding R^2 values are included in brackets). All estimates except that indicated by star are statistically significant at $P < 0.05$.

permafrost soils and its effects on soil carbon dynamics [*Zhuang et al.*, 2001; *Zhu et al.*, 2013a]. The HM has been developed to simulate soil hydrological dynamics and snow cover dynamics [*Zhuang et al.*, 2003; *Tang and Zhuang*, 2011]. The CNDM, which explicitly represents the effects of CO_2 fertilization and nitrogen limitation [*McGuire et al.*, 1992], is used to estimate net CO_2 exchanges (NCE), i.e., the difference between CO_2 uptakes via plant photosynthesis and CO_2 emissions via ecosystem respiration. The MDM, which explicitly represents CH_4 production, oxidation, and transport processes [*Zhuang et al.*, 2004], is used to simulate both CH_4 emissions in wetland ecosystems and CH_4 consumption in upland ecosystems. Since each grid cell may contain both wetland and upland ecosystems, the net CH_4 exchanges (NME, i.e., the difference between CH_4 emissions and consumption) are area-weighted as defined by wetland inundation fraction for each grid cell, which is determined based on simulated grid-cell-mean water table and a TOPMODEL-based saturated topographical wetness index approach [*Zhu et al.*, 2014].

To make spatially explicit estimates of daily ecosystem carbon and snow cover dynamics at each grid cell (0.5° by 0.5°), we used spatially explicit data from different data sources including daily climate forcing (incoming surface shortwave radiation, temperature, precipitation, and relative humidity) simulated by Community Earth System Model under four climate change scenarios (Representative Concentration Pathway (RCP) 2.6, RCP4.5, RCP6.0, and RCP8.5) (http://cmip-pcmdi.llnl.gov/cmip5/data_portal.html) (Table 1), fractional vegetation cover type map from *Euskirchen et al.* [2007], and soil texture from International Soil Reference and Information Centre-World Inventory of Soil Emission Potentials soil database [*Batjes*, 2006]. Vegetation- and soil-specific parameters were taken from our previous studies [*Melillo et al.*, 1993; *Zhuang et al.*, 2004; *Tang and Zhuang*, 2011]. We performed model simulations with transient climate data from 1901 to 2100 with the Climatic Research Unit (CRU) data [*Harris et al.*, 2014] as historical climate forcing (1901–2010). To ensure smooth shifts of climate forcing from historical (1901–2010) to future period (2011–2100), a simple debasing technique was applied to reconcile climate forcing time series from CRU and four climate change scenarios [*Jin et al.*, 2015].

2.3. Calculations of Climate Feedback

Spatially explicit global-mean radiative forcings (RF_{global}) from biogeochemical and biogeophysical effects were all consistently quantified for the purpose of direct comparison: the RF_{global} for a given grid cell, which has units of W m^{-4} (i.e., W m^{-2}/m^2), was calculated as global-mean radiative forcing at the top-of-the-atmosphere (TOA) between 2010 and 2100 arising from biogeochemical and biogeophysical effects in 1 m^2 of grid cell area in that grid cell.

For biogeochemical feedback due to the changes in NME and NCE, RF_{global} for a given grid cell was estimated according to the method of *Frolking et al.* [2006], which considered the combined effect of all past emissions/uptake of CO_2 and CH_4 and the degree to which these gases have dissipated:

$$RF_{global} = \sum_{i=0}^{5} \left(\xi_i A_i f_i \cdot \int_{2010}^{2099} \Phi_i(s) \exp\left(-\frac{2100 - s}{\tau_i} \right) ds \right) \quad (1)$$

where $i = 0 - 4$ is CO_2 and $i = 5$ is CH_4; ξ_i represents a multiplier for indirect effects (1.0 for CO_2 and 1.3 for CH_4); A_i represents the radiative efficiency for CO_2 (0.0198×10^{-13} W m^{-2} kg^{-1}) or CH_4 (1.3×10^{-13} W m^{-2} kg^{-1}); f_i represents the fractional multiplier for different pools for CO_2 (5-pool partition set to be 26%, 24%, 19%, 14%, and 18%, corresponding to adjustment time τ_i of 3, 4, 21, 71, 421, and 10^8 years, respectively) or CH_4

Table 2. The Increase in Surface Atmospheric Heating (Δh) due to the Advance of Snowmelt in Spring (Δh_{sm}) and the Delay of Snow Return in Autumn (Δh_{sr})[a]

Vegetation Cover (Area Percentage)	Δh_{sm} (% of R_S)	Δh_{sr} (% of R_S)
Boreal evergreen needleleaf (24.1%)	20.44	13.26
Dwarf/prostrate shrub tundra (19.8%)	39.34	15.15
Boreal deciduous broadleaf (11.6%)	33.20	11.18
Boreal deciduous needleleaf (11.3%)	32.87	14.68
Grassland/xeric shrubland (11.2%)	21.06	6.86
Low shrub tundra (5.4%)	46.24	14.72
Temperate evergreen needleleaf (2.8%)	29.47	13.18
Temperate deciduous broadleaf/xeric woodland (1.2%)	5.41	5.69

[a]Surface atmospheric heating (h) is defined as the sum of sensible and latent fluxes, and Δh is expressed as observed percentage change in incoming surface shortwave radiation (R_S) for different vegetation types over northern terrestrial ecosystems (north of 50°N) [*Euskirchen et al.*, 2007].

(one pool only with τ_i of 12 years); $\Phi_i(s)$ represents annual net flux of CH_4 or CO_2 at year s; and the integral term is thus cumulative flux of CH_4 or CO_2 by year 2100 after partial decay in the atmosphere.

For biogeophysical feedback due to snow cover and vegetation biomass dynamics, we took a three-step procedure to estimate RF_{global}. First, we calculated grid-cell-mean surface local RFs (RF_{local}) based on the changes in surface energy budget due to the changes in snow cover and vegetation biomass between 2010 and 2100. Second, we used a simple scaling relationship to convert local RFs at the surface into local RFs at TOA [*Lohila et al.*, 2010]: RF_{local} was multiplied by 0.65 to approximately account for the complicated atmospheric effects. Third, local RFs at TOA were area-scaled to global-mean RFs at TOA (i.e., RF_{global}) by dividing the Earth's surface area ($S_E = 5.1 \times 10^{14}\ m^2$).

The RF_{local} due to snow cover dynamics (RF_{local_snow}, $W\ m^{-2}$) was calculated based on simulated snowmelt and snow-return dates, similar to the estimation method used by *Chapin et al.* [2005] and *Euskirchen et al.* [2007]:

$$RF_{local\_snow} = (N_{sm} \times R_{S\_sm} \times \Delta h_{sm}/100 + N_{sr} \times R_{S\_sr} \times \Delta h_{sr}/100)/N_{days} \quad (2)$$

where N_{sm} (N_{sr}) represents the number of days of snowmelt advance in spring (snow return delay in autumn) in 2100 compared to 2010; R_{S_sm} (R_{S_sr}) represents mean incoming surface shortwave radiation (R_S, $W\ m^{-2}$) during snowmelt (snow-return) period; Δh_{sm}(Δh_{sr}) represents grid-cell-mean percentage increase in the ratio of surface atmospheric heating (defined as the sum of sensible and latent fluxes) to R_S due to snowmelt advance (snow return delay). Δh_{sm} and Δh_{sr} are area weighted by the portion of each vegetation cover type in a given half-degree grid cell, and their values for each vegetation cover type (Table 2) were estimated from site observations of the changes in sensible and latent fluxes between presnowmelt and postsnowmelt and between presnow return and postsnow return [*Euskirchen et al.*, 2007]. N_{days} is the number of days of a year (365 or 366).

The RF_{local} due to the increase in vegetation biomass (RF_{local_bio}, $W\ m^{-2}$) was calculated based on simulated vegetation biomass:

$$RF_{local\_bio} = (N_{grow} \times R_{S\_grow} \times \Delta h_{grow}/100)/N_{days} \quad (3)$$

where N_{grow} represents simulated mean growing season length (days) over 2011–2100, R_{S_grow} represents mean R_S during growing season over 2011–2100, and Δh_{grow} represents the percentage increase in the ratio of surface atmospheric heating to R_S due to the increase in vegetation biomass. Due to the lack of information on the relationship between heat fluxes and vegetation biomass, Δh_{grow} was approximately set as the change in surface albedo during growing season ($\Delta\alpha_{grow}$), which was estimated from vegetation biomass following an empirical biomass-albedo relationship developed in NTEs [*Thompson et al.*, 2004]: 0.024 decrease in α_{grow} corresponds to 1 kg C m^{-2} increase in vegetation aboveground biomass. Since TEM only simulates total vegetation biomass, aboveground biomass was estimated from TEM-simulated total biomass based on aboveground/belowground net primary production (NPP) partition patterns [*Gill and Jackson*, 2003], by assuming that biomass shares the same aboveground/belowground partition patterns as NPP. It should be mentioned that we averaged annual shortwave RF arising from the changes in snow cover and vegetation biomass over the whole year ($N_{days} = 365$ or 366), instead of a 90 day summer season as used in *Chapin et al.* [2005] and *Euskirchen et al.* [2007], in order to represent annual-mean climate feedback.

3. Results

3.1. Changes in Net CH_4 Exchange

Corresponding to projected climate change over 2011–2100 (Table 1), the magnitude of TEM-simulated annual NME across NTEs generally increased (Figure 1). The magnitude of annual NME increase differed among climate change scenarios with strongest and weakest increases in RCP8.5 and RCP2.6 scenarios, respectively, while the spatial patterns of annual NME change were similar across different scenarios. Obvious changes in annual NME came from stronger CH_4 emissions from high-emitting areas (up to an increase of 6 g CH_4 m^{-2} yr^{-1} between the 2010s and 2090s under RCP8.5 scenario), mainly located in western Siberia and northern Canada where wetlands are extensively distributed. Under four climate change scenarios, regional annual NME by 2100 was projected to have an increase of 17.8–49.9 Tg CH_4, accounting for 33–92% of regional annual NME in 2010 (54.3 Tg CH_4 yr^{-1}) (Table 3). By aggregating temporally the differences in annual NME between 2010 and subsequent years and then aggregating spatially over NTEs (total vegetated area: 2.94×10^7 km^2), we calculated that the region as a whole will emit additional 0.8–2.2 Pg CH_4 into the atmosphere due to climate change over 2011–2100, and therefore provide an NME-induced positive climate feedback (i.e., a heating effect).

3.2. Changes in Net CO_2 Exchange

Similar to annual NME, the magnitude of annual NCE over NTEs were projected to increase over 2011–2100 across climate change scenarios (Figure 2; negative changes in annual NCE denoted stronger sinks or weaker sources). In general, more CO_2 was sequestered by northern terrestrial ecosystems over 2011–2100 with more obvious change for RCP4.5 and RCP6.0 scenarios (up to -16 g C m^{-2} yr^{-1} between the 2010s and 2090s; a cooling effect). Although the projected change in annual NCE was spatially heterogeneous, warmer terrestrial ecosystems in southern parts of NTEs seemed to exert a stronger cooling effect (more negative change in annual NCE) compared to colder areas in northern parts. The region as a whole acted as a weak CO_2 sink of -0.52 Pg C yr^{-1} in 2010, and this sink was projected to have an increase of 0.12–0.22 Pg C by 2100 under four climate change scenarios (23–42% of regional sink in 2010) (Table 3). By integrating temporally and spatially the changes in annual NCE, we projected that the region as a whole will sequestrate additional 5.5–10.1 Pg C due to climate change over 2011–2100, and therefore provide an NCE-induced negative climate feedback (i.e., a cooling effect).

3.3. Snow Cover Dynamics

Driven by projected climate change over 2011–2100, our model generally simulated earlier snowmelt in spring (Figure S1 in the supporting information) and later snow return in autumn (Figure S2) over NTEs, both of which led to a shorter snow cover duration or a longer snow-free season length (SFL) (Figure 3). For snowmelt dynamics in spring, some areas (e.g., western part of Europe) experienced strong snowmelt advance, while other areas generally experienced moderate snowmelt advance (Figure S1). For snow return dynamics, most evident change was located in central Siberia (Figure S2). We estimated regional mean snowmelt and snow return dates in 2010 as 170.5 and 286.7 (day of year), respectively, and we projected that climate change over 2011–2100 will lead to an advance in snowmelt date of 6.2–20.3 days and a delay in snow return date of 5.5–21.4 days by 2100 under four climate change scenarios (Table 3). Taken together, we projected an increase in SFL over 2011–2100 in most areas (Figure 3) with an increase of 11.7–41.7 days by 2100 in regional mean SFL (Table 3). The projected increase in SFL led to a decrease in surface albedo and an increase in radiation absorption (during snow-melt advance and snow return periods). Therefore, NTEs will provide a heating effect over 2011–2100, attributed to the change of snow cover dynamics with climate change.

3.4. Vegetation Biomass Carbon Dynamics

Vegetation biomass carbon (VEC) in NTEs was consistently projected to increase under four climate change scenarios but with different increasing rates (Figure 4). The increase in VEC between the 2010s and 2090s was smallest (up to 200 g C m^{-2}) and largest (up to 800 g C m^{-2}) under RCP2.6 and RCP8.5 scenarios, respectively. Compared to NME, NCE, and SFL dynamics, the increase in VEC was more spatially homogeneous over the region. We projected that climate change over 2011–2100 will lead to an increase in regional mean VEC of 104.8–498.7 g C m^{-2} by 2100 under four climate change scenarios (Table 3). Since surface albedo was inversely correlated with VEC, the increase in VEC led to a decrease in surface albedo. Therefore, our simulations indicated that NTEs will provide a VEC-induced heating effect over 2011–2100.

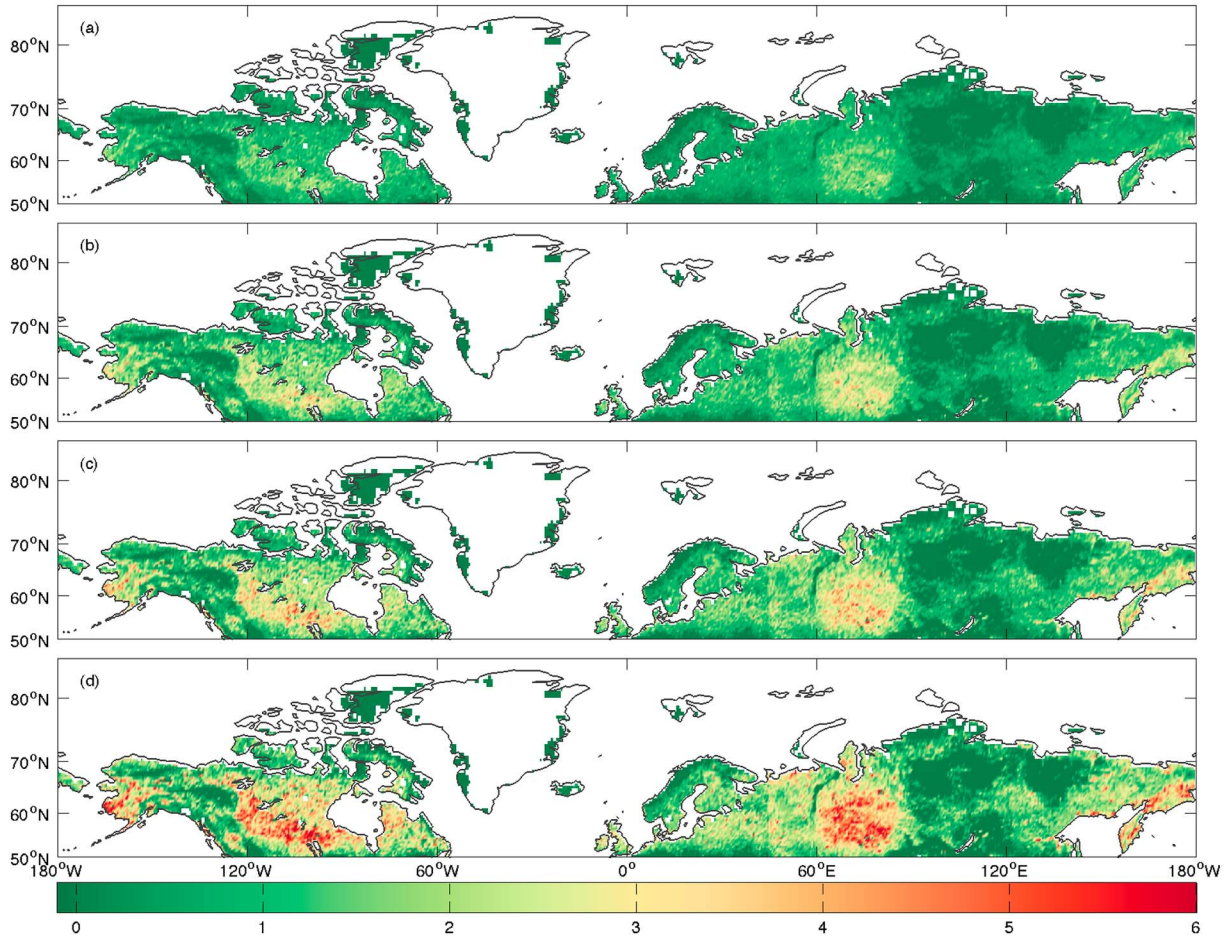

Figure 1. Change in decadal mean annual net CH_4 exchanges (NME, g CH_4 m^{-2} yr^{-1}) between the 2010s and 2090s ($\overline{NME_{2090s}} - \overline{NME_{2010s}}$) over northern terrestrial ecosystems (north of 50°N), under four climate change scenarios: (a) RCP2.6, (b) RCP4.5, (c) RCP6.0, and (d) RCP8.5. Positive values indicate stronger sources or weaker sinks, and negative values indicate stronger sinks or weaker sources.

Table 3. Changes in Regional Model Predications Over Northern Terrestrial Ecosystems (North of 50°N), Between 2010 and 2100 Under Four Climate Change Scenarios[a]

		Δ (2100–2010)			
	2010	RCP2.6	RCP4.5	RCP6.0	RCP8.5
NME (Tg CH_4 yr^{-1})	54.3	17.8	28.5	35.7	49.9
NPP (Pg C yr^{-1})	−5.29	−0.41	−0.82	−1.02	−1.63
RH (Pg C yr^{-1})	4.77	0.28	0.62	0.80	1.51
NCE (Pg C yr^{-1})	−0.52	−0.13	−0.20	−0.22	−0.12
Snowmelt date (days)	170.5[b]	−6.2	−10.8	−15.2	−20.3
Snow return date (days)	286.7[b]	5.5	9.9	13.0	21.4
Snow-free season length (days)	142.6	11.7	20.7	28.2	41.7
Vegetation biomass carbon (g C m^{-2})	1438.2	104.8	256.5	317.9	498.7

[a]Net CH_4 exchange (NME), net primary production (NPP), heterotrophic respiration (RH), and net CO_2 exchange (NCE) are spatially aggregated values over the region with positive and negative values which denote sources and sinks, respectively, while snow cover dynamics and vegetation biomass carbon are spatially averaged values over the region.
[b]Snowmelt and snow return dates for 2010 are expressed as day of year.

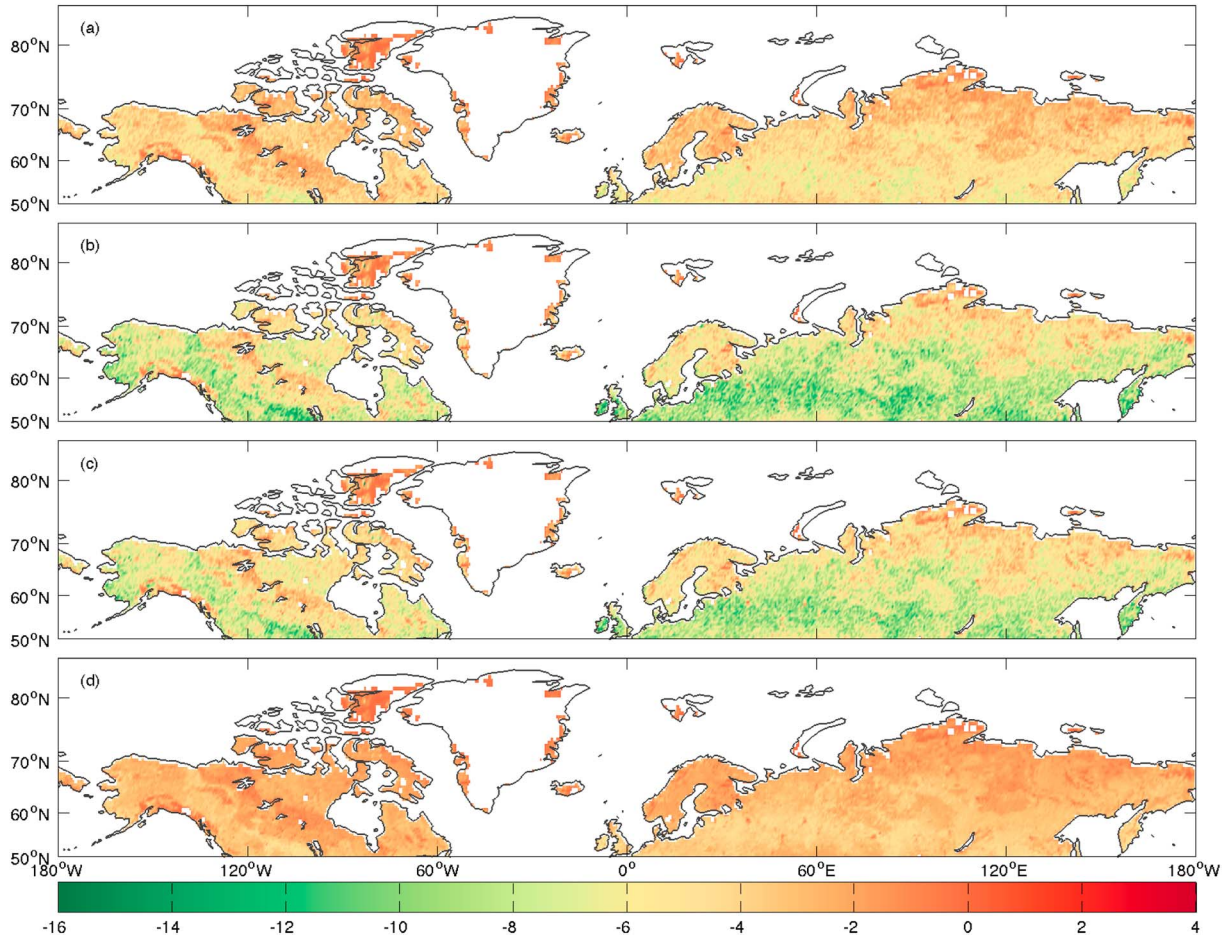

Figure 2. Change in decadal mean annual net CO_2 exchanges (NCE, $g\,C\,m^{-2}\,yr^{-1}$) between the 2010s and 2090s ($\overline{NCE_{2090s}} - \overline{NCE_{2010s}}$) over northern terrestrial ecosystems (north of 50°N), under four climate change scenarios: (a) RCP2.6, (b) RCP4.5, (c) RCP6.0, and (d) RCP8.5. Positive values indicate stronger sources or weaker sinks, and negative values indicate stronger sinks or weaker sources.

3.5. Climate Feedback

By consistently expressing biogeochemical and biogeophysical feedback as global-mean radiative forcing at TOA between 2010 and 2100 (RF_{global}), we calculated spatially explicit RF_{global} over NTEs arising from the changes in NME, NCE, SFL, and VEC (Figure 5). The RF_{global} showed strong spatial variations over the region, with a cooling effect (up to $-1\times10^{-14}\,W\,m^{-4}$) for some areas and a heating effect for others (up to $4\times10^{-14}\,W\,m^{-4}$). Across four climate change scenarios, the spatial patterns of RF_{global} did not change evidently, although the magnitude of RF_{global} increased from low- to high-emission scenarios. Among the four components of RF_{global} (i.e., NME, NCE, SFL, and VEC), the spatial pattern of RF_{global} resembled more to those of SFL (Figure 3) and NME (Figure 1).

We projected that NTEs as a whole will exert a heating effect on the atmosphere and that the regional aggregated RF_{global} between 2010 and 2100 will be 0.04–0.26 $W\,m^{-2}$ with increasing RF_{global} from low- to high-emission scenarios (Figure 6). Among four components of RF_{global}, NME, SFL, and VEC exerted a heating effect while NCE exerted a cooling effect. In terms of absolute magnitude of these components, RF_{global} was more attributed to SFL and NME. Across four climate change scenarios, the heating effects from NME, SFL, and VEC increased from low- to high-emission scenarios, while the cooling effect from NCE increased from RCP2.6 to RCP6.0 and then, for RCP8.5, returned to a level close to RCP2.6.

4. Discussion

Our estimate of contemporary regional CH_4 emissions from NTEs, 54.3 $Tg\,CH_4\,yr^{-1}$ in 2010, is within the range of previous regional estimates of CH_4 emissions, 20–157 $Tg\,CH_4\,yr^{-1}$, from similar study domains

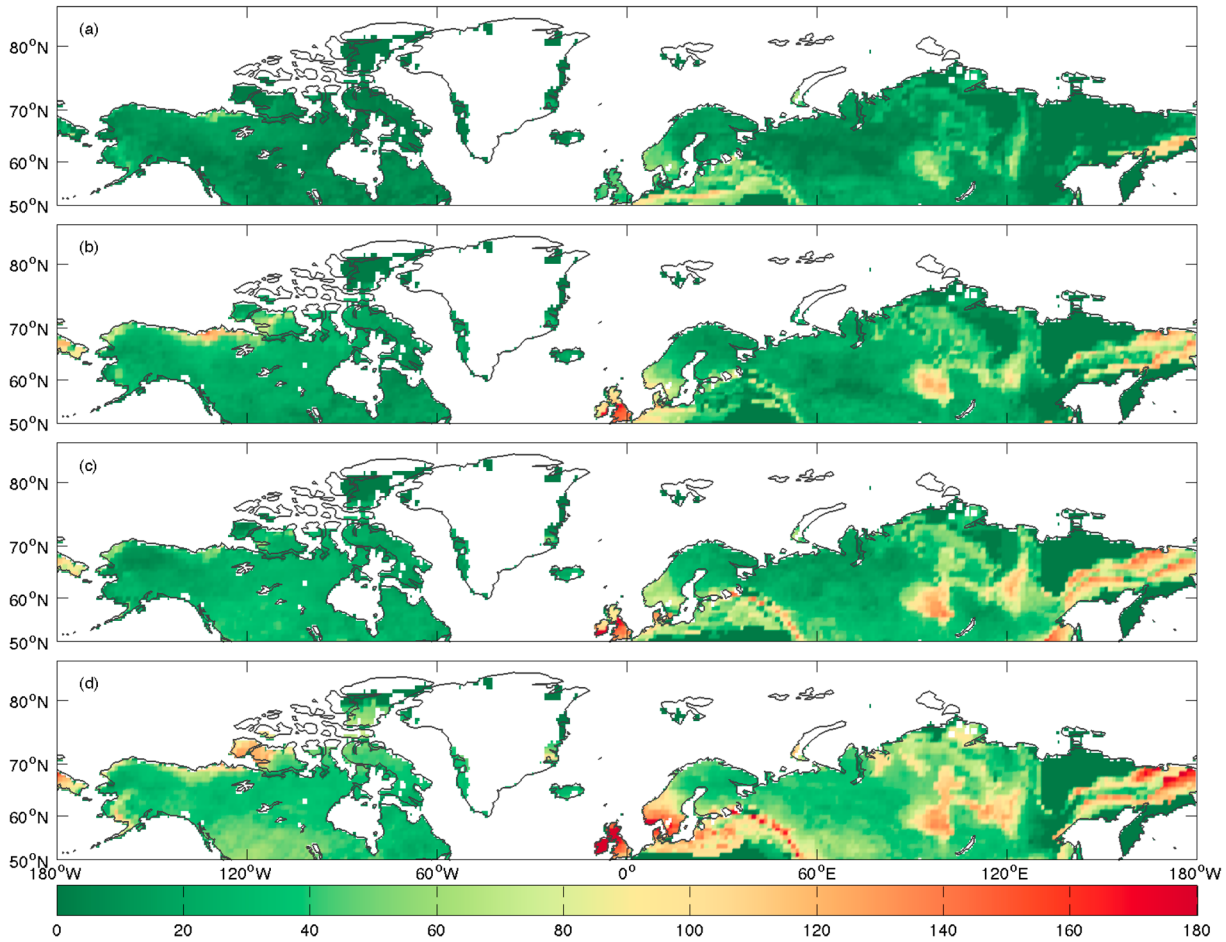

Figure 3. Increase in decadal mean snow-free season length (SFL, days) between the 2010s and 2090s $\left(\overline{SFL_{2090s}} - \overline{SFL_{2010s}}\right)$ over northern terrestrial ecosystems (north of 50°N), under four climate change scenarios: (a) RCP2.6, (b) RCP4.5, (c) RCP6.0, and (d) RCP8.5.

[*Christensen et al.*, 1996; *Zhuang et al.*, 2004; *Petrescu et al.*, 2010; *Zhu et al.*, 2013b]. Consistent with previous modeling studies [*Anisimov*, 2007; *Koven et al.*, 2011], our model simulates an increasing CH_4 source in response to future climate change over this century. In accordance with the projections by *Gedney et al.* [2004] and *Zhuang et al.* [2006], we also project a doubling of CH_4 emissions by the end of this century when anthropogenic emissions are high (RCP8.5). Our estimate of contemporary regional CO_2 sink, $-0.52\,Pg\,C\,yr^{-1}$ in 2010, is also comparable to previous estimates of CO_2 sink for similar study domain, -0.8–$0\,Pg\,C\,yr^{-1}$ [*McGuire et al.*, 2009; *Koven et al.*, 2011; *Schaphoff et al.*, 2013]. Our projections of regional CO_2 sink in 2100, -0.65 to $-0.74\,Pg\,C\,yr^{-1}$, are slightly larger than the multimodel estimates by *Qian et al.* [2010] $(0.3 \pm 0.3\,Pg\,C\,yr^{-1})$. Although climate change under all four scenarios will result in an increasing regional CO_2 sink since NPP is rising faster than RH (Table 3), there will not be a consistent relationship between the extent of increase in CO_2 sink and the extent of climate change. A stronger climate change corresponds to a larger increase in CO_2 sink for RCP2.6, RCP4.5, and RCP6.0 scenarios; however, the strongest climate change scenario (RCP8.0) leads to the smallest increase in CO_2 sink (Table 3). This inconsistent relationship is caused by differential responses of NPP and RH to climate change, which may result in gradually decreasing difference between NPP and RH [*Koven et al.*, 2011; *Zhang et al.*, 2014]. For example, we project a larger difference in RH in 2100 between RCP6.0 and RCP8.5 $(0.71\,Pg\,C\,yr^{-1})$ than the difference in NPP $(0.61\,Pg\,C\,yr^{-1})$, which explains why the increase in CO_2 sink by 2100 is smaller under RCP8.5 than RCP6.0 (Table 3).

Our projection of climate-induced changes in snow cover dynamics in NTEs generally agrees with other studies [*Dye*, 2002; *Stone et al.*, 2002; *Euskirchen et al.*, 2007]. During the last three decades of last century,

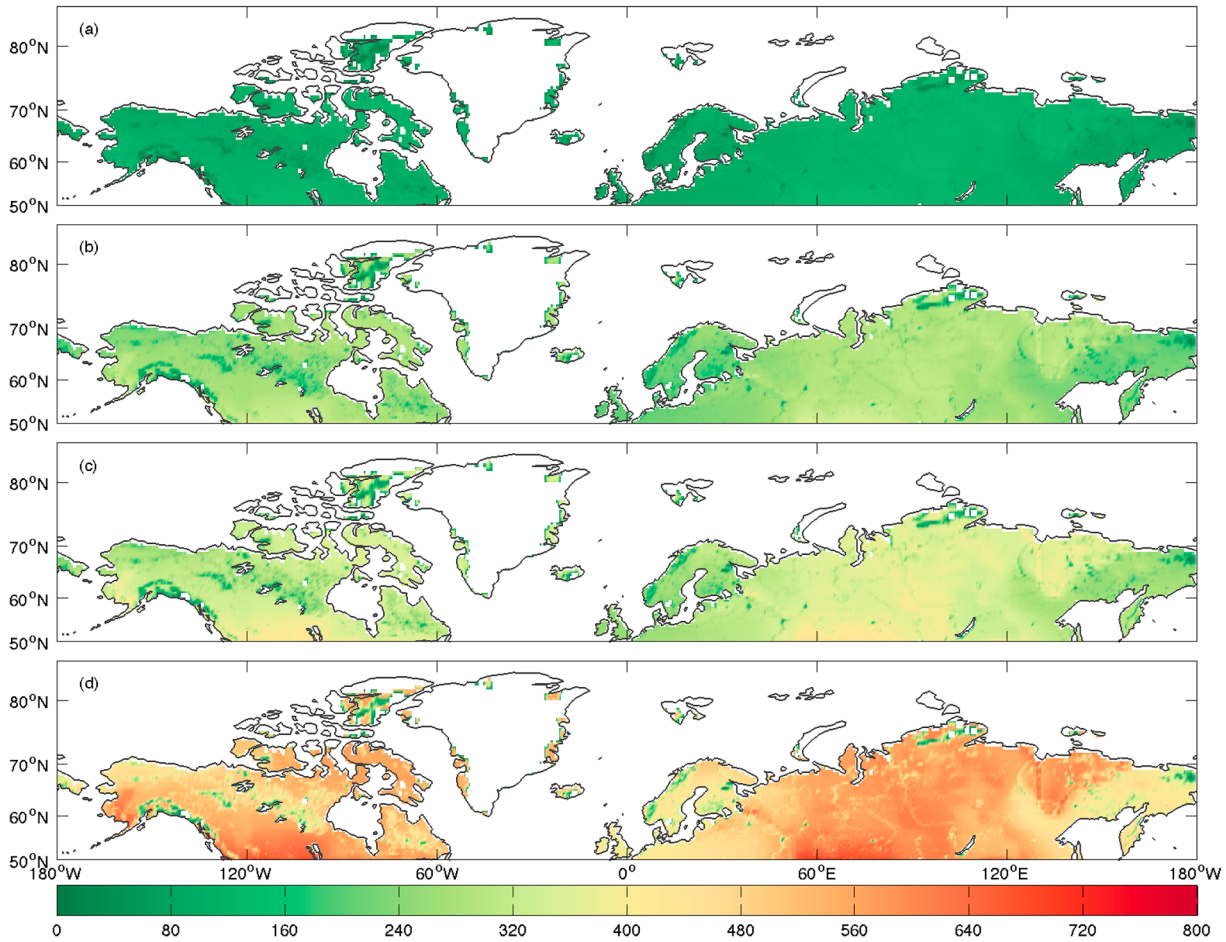

Figure 4. Increase in decadal mean vegetation carbon (VEC, g C m^{-2}) between the 2010s and 2090s ($\overline{VEC_{2090s}} - \overline{VEC_{2010s}}$) over northern terrestrial ecosystems (north of 50°N), under four climate change scenarios: (a) RCP2.6, (b) RCP4.5, (c) RCP6.0, and (d) RCP8.5.

Euskirchen et al. [2007] estimated an increase in regional mean SFL of 0.22 d yr^{-1} over the same study domain, and *Dye* [2002] estimated an increase of 0.5–0.6 d yr^{-1} over the region north of 45°N. Taking the RCP4.5 sceanrio, which has a similar warming trend (0.04°C yr^{-1}) as in those three decades, for comparison, we project an increase in regional mean SFL of 0.23 d yr^{-1} (earlier snowmelt of 0.12 d yr^{-1} and delayed snow return of 0.11 d yr^{-1}) over 2011–2100, which is close to the estimate by *Euskirchen et al.* [2007] but smaller than *Dye* [2002]. Although the changes in snowmelt and snow return dates are about the same, RF will be more attributed to snowmelt advance in spring than snow return delay in autumn. This difference is due to asymmetric solar radiation input during snowmelt and snow return periods in northern hemisphere, where snowmelt periods (around 170.5, day of year; close to summer solstice) receive more radiation input than snow return periods (around 286.7, day of year; between the autumn equinox and winter solstice) (Table 3). The extent of climate-induced increase in vegetation biomass carbon by 2100 co-varies with the extent of climate change, with larger carbon increase corresponding to stronger climate change. The projected regional mean vegetation carbon increases by 2100 (104.8–498.7 g C m^{-2}) are comparable to a model ensemble projection of vegetation carbon increase (141.9–328.3 g C m^{-2}) in northern Alaska [*Euskirchen et al.*, 2009]. Among those climate forcing variables (Table 1), the extent of increase in vegetation biomass matches best with the extent of increase in air temperature.

Under present climate conditions, NTEs as a whole act as a CH_4 source and a CO_2 sink. Although CH_4 source in 2010 is 1 order of magnitude smaller than CO_2 sink, its much higher radiative efficiency warrants the importance of CH_4 emissions in determining regional warming potential. With climate change over

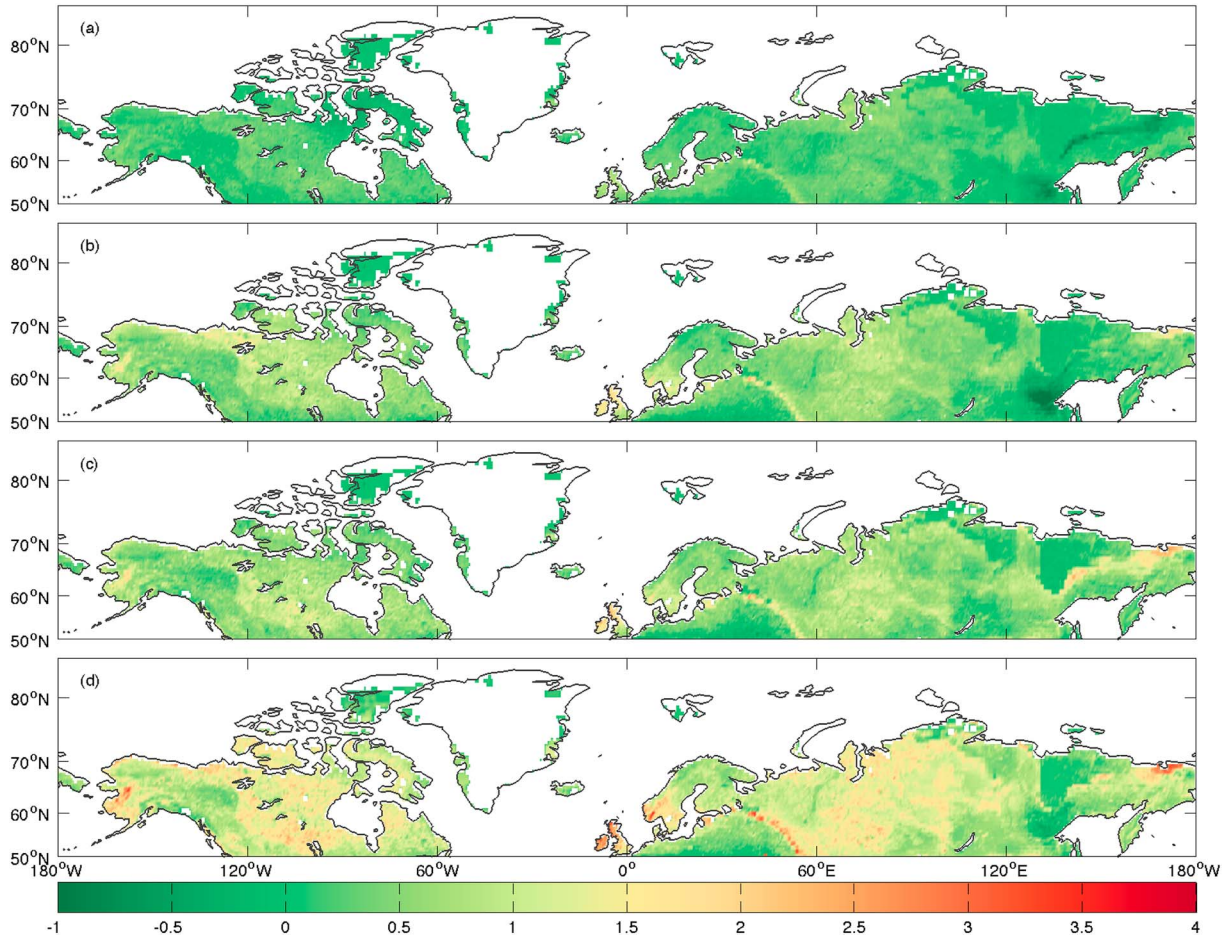

Figure 5. Global-mean net radiative forcing ($W\,m^{-4} \times 10^{-14}$) at the top-of-the-atmosphere between 2010 and 2100 arising from both biogeochemical and biogeophysical effects over northern terrestrial ecosystems (north of 50°N), under four climate change scenarios: (a) RCP2.6, (b) RCP4.5, (c) RCP6.0, and (d) RCP8.5.

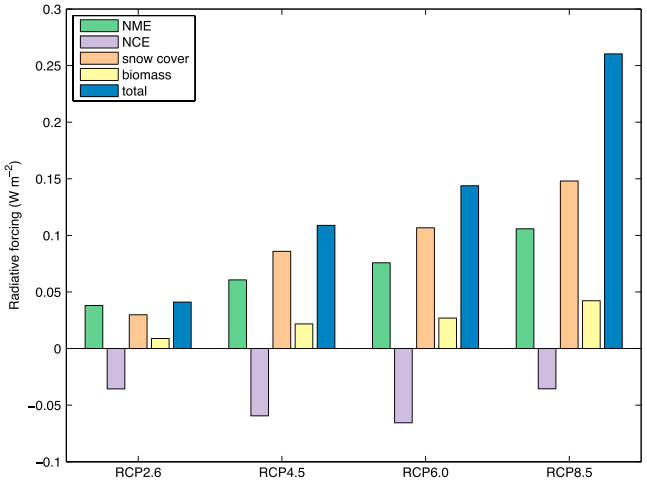

Figure 6. Global-mean radiative forcing ($W\,m^{-2}$) at the top-of-the-atmosphere between 2010 and 2100 due to the changes in net CH_4 exchanges (NME), net CO_2 exchanges (NCE), snow cover retreat, and vegetation biomass under four climate change scenarios: RCP2.6, RCP4.5, RCP6.0, and RCP8.5. The values represent spatial aggregation of global-mean radiative forcing over northern terrestrial ecosystems (north of 50°N).

2011–2100, this warming potential will become larger since CH_4 source increases faster than CO_2 sink. The positive and negative RFs induced by larger CH_4 source and CO_2 sink, respectively, indicate that NTEs will exert an NME-induced positive feedback and an NCE-induced negative feedback to the atmosphere. Since NME-induced positive feedback is consistently larger than NCE-induced negative feedback across climate change scenarios, the region will exert a positive net biogeochemical feedback of 0.002–0.07 $W\,m^{-2}$. On the other hand, both longer SFL and larger VEC cause positive RF, and thus, the region will exert a positive biogeophysical feedback of 0.04–0.19 $W\,m^{-2}$, which is much larger than biogeochemical feedback. Taken together, NTEs will exert a

positive net RF of 0.04–0.26 W m^{-2}, suggesting that climate-induced structural and functional changes of NTEs will result in net climate warming. This positive net RF from NTEs will be smaller in comparison with RF arising from projected anthropogenic CO_2 emissions by 2100, which will be 0.3–6.2 W m^{-2} relative to year 2010 if we consider RCP scenarios. Our estimation of positive net RF is consistent with the findings in previous large-scale afforestation model experiments [e.g., *Betts*, 2000; *Gibbard et al.*, 2005; *Arora and Montenegro*, 2011]; however, it is noted that our conclusion is based on climate-induced realistic and transient land surface dynamics instead of idealized land cover transition as in those afforestation model experiments. We also find that by excluding the CH_4-related positive RF, net RF reduces by 41–93%, which confirms the importance of the CH_4-related RF in regulating ecosystem-climate feedback and implies previous studies without considering that the CH_4-related biogeochemical RF might have underestimated the intensity of total terrestrial feedback to the climate system in northern high latitudes.

Although our climate-uncoupled model simulations are relatively simple compared to fully climate-coupled simulations with Integrated Earth System Models, our model-based feedback estimations still suffer from many potential error sources. In addition to common uncertainties pertaining to modeling studies such as imperfect model structures and incomplete model parameterization, there are several uncertainties in our estimations of terrestrial feedback. One of these uncertainties arises from the procedure we used to calculate global-mean RFs arising from the changes in NME and NCE. Although the method proposed by *Frolking et al.* [2006] might perform better than standard GWP approach especially when accounting for multiple sustained GHG fluxes with different radiative efficiencies, some of the assumptions of Frolking's method are still open to debate, such as constant background atmosphere assumption, different pool settings [*Joos et al.*, 2013], and different values of the multiplier of the indirect effect of CH_4 [*Stocker et al.*, 2013]. Further tests are needed in future to examine these effects on our RF estimations. Another source of uncertainty comes from the method we used to calculate RF due to warming-induced increase in vegetation biomass. Due to the lack of empirical data, we only consider RF from reduced albedo with growing vegetation without RF from the change in surface energy partitioning pattern. Increased vegetation biomass may also lead to higher surface roughness, and therefore accelerated transport of latent fluxes into the atmosphere, resulting in a negative feedback. Accordingly, our estimation of VEC-induced RF might be overestimated by disregarding this negative feedback. In addition, we neglect some other mechanisms that are potentially important for quantifying ecosystem-climate feedback in northern high latitudes, such as vegetation shifts [*Wilmking et al.*, 2004] and fire disturbances [*Carrasco et al.*, 2006]. Further assessments of the impacts of these missing mechanisms on ecosystem-climate feedback are needed.

Acknowledgments

This research is supported with funded projects to Q.Z. by NASA Land Use and Land Cover Change program (NASA NNX09AI26G), Department of Energy (DE-FG02-08ER64599), National Science Foundation (NSF-1028291 and NSF-0919331), and the NSF Carbon and Water in the Earth Program (NSF-0630319), as well as funded projects to X.Z. by Open Fund of State Key Laboratory of Remote Sensing Science of China (OFSLRSS201501) and by the Fundamental Research Funds for the Central Universities of China (20720160109). To obtain the model simulation data of this study, send request to Q.Z. (qzhuang@purdue.edu).

References

Anisimov, O. A. (2007), Potential feedback of thawing permafrost to the global climate system through methane emission, *Environ. Res. Lett.*, *2*(4), 045016, doi:10.1088/1748-9326/2/4/045016.

Arora, V. K., and A. Montenegro (2011), Small temperature benefits provided by realistic afforestation efforts, *Nat. Geosci.*, *4*(8), 514–518.

Bala, G., K. Caldeira, A. Mirin, M. Wickett, C. Delire, and T. J. Phillips (2006), Biogeophysical effects of CO_2 fertilization on global climate, *Tellus, Ser. B*, *58*(5), 620–627.

Bathiany, S., M. Claussen, V. Brovkin, T. Raddatz, and V. Gayler (2010), Combined biogeophysical and biogeochemical effects of large-scale forest cover changes in the MPI earth system model, *Biogeosciences*, *7*(5), 1383–1399, doi:10.5194/bg-7-1383-2010.

Batjes, N. H. (2006), ISRIC-WISE derived soil properties on a 5 by 5 arc-minutes global grid (version 1.0), ISRIC—World Soil Information, Wageningen.

Betts, R. A. (2000), Offset of the potential carbon sink from boreal forestation by decreases in surface albedo, *Nature*, *408*(6809), 187–190.

Betts, R. A., P. D. Falloon, K. K. Goldewijk, and N. Ramankutty (2007), Biogeophysical effects of land use on climate: Model simulations of radiative forcing and large-scale temperature change, *Agric. For. Meteorol.*, *142*(2), 216–233.

Bonan, G. B. (2008), Forests and climate change: Forcings, feedbacks, and the climate benefits of forests, *Science*, *320*(5882), 1444–1449.

Bonfils, C. J. W., T. J. Phillips, D. M. Lawrence, P. Cameron-Smith, W. J. Riley, and Z. M. Subin (2012), On the influence of shrub height and expansion on northern high latitude climate, *Environ. Res. Lett.*, *7*(1), 015503.

Brovkin, V., M. Claussen, E. Driesschaert, T. Fichefet, D. Kicklighter, M. F. Loutre, H. D. Matthews, N. Ramankutty, M. Schaeffer, and A. Sokolov (2006), Biogeophysical effects of historical land cover changes simulated by six earth system models of intermediate complexity, *Clim. Dyn.*, *26*(6), 587–600, doi:10.1007/s00382-005-0092-6.

Carrasco, J. J., J. C. Neff, and J. W. Harden (2006), Modeling physical and biogeochemical controls over carbon accumulation in a boreal forest soil, *J. Geophys. Res.*, *111*, G02004, doi:10.1029/2005JG000087.

Chapin, F. S., M. Sturm, M. C. Serreze, J. P. McFadden, J. R. Key, A. H. Lloyd, A. D. McGuire, T. S. Rupp, A. H. Lynch, and J. P. Schimel (2005), Role of land-surface changes in Arctic summer warming, *Science*, *310*(5748), 657–660.

Christensen, T. R., I. C. Prentice, J. Kaplan, A. Haxeltine, and S. Sitch (1996), Methane flux from northern wetlands and tundra, *Tellus, Ser. B*, *48*(5), 652–661.

Claussen, M., V. Brovkin, and A. Ganopolski (2001), Biogeophysical versus biogeochemical feedbacks of large-scale land cover change, *Geophys. Res. Lett.*, *28*, 1011–1014, doi:10.1029/2000GL012471.

Comiso, J. C., and D. K. Hall (2014), Climate trends in the Arctic as observed from space, *Wiley Interdiscip. Rev.: Clim. Change*, *5*, 389–409, doi:10.1002/wcc.277.

Dye, D. G. (2002), Variability and trends in the annual snow-cover cycle in Northern Hemisphere land areas, 1972–2000, *Hydrol. Processes*, *16*(15), 3065–3077, doi:10.1002/hyp.1089.
Euskirchen, E. S., A. D. McGuire, and F. S. Chapin (2007), Energy feedbacks of northern high-latitude ecosystems to the climate system due to reduced snow cover during 20th century warming, *Global Change Biol.*, *13*(11), 2425–2438.
Euskirchen, E. S., A. D. McGuire, F. S. Chapin Iii, S. Yi, and C. C. Thompson (2009), Changes in vegetation in northern Alaska under scenarios of climate change, 2003–2100: Implications for climate feedbacks, *Ecol. Appl.*, *19*(4), 1022–1043.
Field, C. B., D. B. Lobell, H. A. Peters, and N. R. Chiariello (2007), Feedbacks of terrestrial ecosystems to climate change, *Annu. Rev. Environ. Resour.*, *32*(1), 1–29, doi:10.1146/annurev.energy.32.053006.141119.
Friedlingstein, P., P. Cox, R. Betts, L. Bopp, W. Von Bloh, V. Brovkin, P. Cadule, S. Doney, M. Eby, and I. Fung (2006), Climate-carbon cycle feedback analysis: Results from the C4MIP model intercomparison, *J. Clim.*, *19*(14), 3337–3353.
Frolking, S., N. Roulet, and J. Fuglestvedt (2006), How northern peatlands influence the Earth's radiative budget: Sustained methane emission versus sustained carbon sequestration, *J. Geophys. Res.*, *111*, G01008, doi:10.1029/2005JG000091.
Gedney, N., P. M. Cox, and C. Huntingford (2004), Climate feedback from wetland methane emissions, *Geophys. Res. Lett.*, *31*, L20503, doi:10.1029/2004GL020919.
Gibbard, S., K. Caldeira, G. Bala, T. J. Phillips, and M. Wickett (2005), Climate effects of global land cover change, *Geophys. Res. Lett.*, *32*, L23705, doi:10.1029/2005GL024550.
Gill, R., and R. B. Jackson (2003), Global distribution of root turnover in terrestrial ecosystems, Oak Ridge Natl. Lab. Distributed Active Arch. Cent., Oak Ridge, Tenn., doi:10.3334/ORNLDAAC/661.
Harris, I., P. D. Jones, T. J. Osborn, and D. H. Lister (2014), Updated high-resolution grids of monthly climatic observations - The CRU TS3.10 dataset, *Int. J. Climatol.*, *34*(3), 623–642, doi:10.1002/joc.3711.
Jin, Z., Q. Zhuang, J.-S. He, X. Zhu, and W. Song (2015), Net exchanges of methane and carbon dioxide on the Qinghai-Tibetan Plateau from 1979 to 2100, *Environ. Res. Lett.*, *10*(8), 085007.
Joos, F., R. Roth, J. S. Fuglestvedt, G. P. Peters, I. G. Enting, W. von Bloh, V. Brovkin, E. J. Burke, M. Eby, and N. R. Edwards (2013), Carbon dioxide and climate impulse response functions for the computation of greenhouse gas metrics: A multi-model analysis, *Atmos. Chem. Phys.*, *13*(5), 2793–2825.
Koven, C. D., B. Ringeval, P. Friedlingstein, P. Ciais, P. Cadule, D. Khvorostyanov, G. Krinner, and C. Tarnocai (2011), Permafrost carbon-climate feedbacks accelerate global warming, *Proc. Natl. Acad. Sci. U.S.A.*, *108*(36), 14,769–14,774.
Lohila, A., K. Minkkinen, J. Laine, I. Savolainen, J.-P. Tuovinen, L. Korhonen, T. Laurila, H. Tietäväinen, and A. Laaksonen (2010), Forestation of boreal peatlands: Impacts of changing albedo and greenhouse gas fluxes on radiative forcing, *J. Geophys. Res.*, *115*, G04011, doi:10.1029/2010JG001327.
McGuire, A. D., J. M. Melillo, L. A. Joyce, D. W. Kicklighter, A. L. Grace, B. Moore Iii, and C. J. Vorosmarty (1992), Interactions between carbon and nitrogen dynamics in estimating net primary productivity for potential vegetation in North America, *Global Biogeochem. Cycles*, *6*, 101–124, doi:10.1029/92GB00219.
McGuire, A. D., L. G. Anderson, T. R. Christensen, S. Dallimore, L. Guo, D. J. Hayes, M. Heimann, T. D. Lorenson, R. W. Macdonald, and N. Roulet (2009), Sensitivity of the carbon cycle in the Arctic to climate change, *Ecol. Monogr.*, *79*(4), 523–555, doi:10.1890/08-2025.1.
McGuire, A. D., et al. (2010), An analysis of the carbon balance of the Arctic Basin from 1997 to 2006, *Tellus, Ser. B*, *62*(5), 455–474, doi:10.1111/j.1600-0889.2010.00497.x.
McGuire, A. D., et al. (2012), An assessment of the carbon balance of Arctic tundra: Comparisons among observations, process models, and atmospheric inversions, *Biogeosciences*, *9*(8), 3185–3204, doi:10.5194/bg-9-3185-2012.
Melillo, J. M., A. D. McGuire, D. W. Kicklighter, B. Moore, C. J. Vorosmarty, and A. L. Schloss (1993), Global climate change and terrestrial net primary production, *Nature*, *363*(6426), 234–240.
Petrescu, A. M. R., L. P. H. van Beek, J. van Huissteden, C. Prigent, T. Sachs, C. A. R. Corradi, F. J. W. Parmentier, and A. J. Dolman (2010), Modeling regional to global CH4 emissions of boreal and arctic wetlands, *Global Biogeochem. Cycles*, *24*, GB4009, doi:10.1029/2009GB003610.
Piao, S., P. Friedlingstein, P. Ciais, N. Viovy, and J. Demarty (2007), Growing season extension and its impact on terrestrial carbon cycle in the Northern Hemisphere over the past 2 decades, *Global Biogeochem. Cycles*, *21*, GB3018, doi:10.1029/2006GB002888.
Pieter, S. A. B., and J. G. Scott (2011), Satellite observations of high northern latitude vegetation productivity changes between 1982 and 2008: Ecological variability and regional differences, *Environ. Res. Lett.*, *6*(4), 045,501.
Polyakov, I., G. Alekseev, R. Bekryaev, U. Bhatt, R. Colony, M. Johnson, V. Karklin, A. Makshtas, D. Walsh, and A. Yulin (2002), Observationally based assessment of polar amplification of global warming, *Geophys. Res. Lett.*, *29*(18), 1878, doi:10.1029/2001GL011111.
Qian, H., R. Joseph, and N. Zeng (2010), Enhanced terrestrial carbon uptake in the northern high latitudes in the 21st century from the Coupled Carbon Cycle Climate Model Intercomparison Project model projections, *Global Change Biol.*, *16*(2), 641–656, doi:10.1111/j.1365-2486.2009.01989.x.
Raich, J. W., E. B. Rastetter, J. M. Melillo, D. W. Kicklighter, P. A. Steudler, B. J. Peterson, A. L. Grace, B. M. Iii, and C. J. Vörösmarty (1991), Potential net primary productivity in South America: Application of a global model, *Ecol. Appl.*, *1*(4), 399–429.
Romanovsky, V. E., T. E. Osterkamp, T. S. Sazonova, N. I. Shender, and V. T. Balobaev (2000), Past and future changes in permafrost temperatures along the East Siberian transect and an Alaskan transect, *Eos Trans. AGU*, *81*(48), F223–F224.
Schaphoff, S., U. Heyder, S. Ostberg, D. Gerten, J. Heinke, and W. Lucht (2013), Contribution of permafrost soils to the global carbon budget, *Environ. Res. Lett.*, *8*(1), 014026.
Stocker, T. F., Q. Dahe, and G.-K. Plattner (2013), Summary for policymakers, in *Climate Change 2013: The Physical Science Basis, Working Group I Contribution to the Fifth Assessment Report of the Intergovernmental Panel on Climate Change*, pp. 3–29, Cambridge Univ. Press, Cambridge, U. K.
Stone, R. S., E. G. Dutton, J. M. Harris, and D. Longenecker (2002), Earlier spring snowmelt in northern Alaska as an indicator of climate change, *J. Geophys. Res.*, *107*(D10), 4089, doi:10.1029/2000JD000286.
Tang, J., and Q. Zhuang (2011), Modeling soil thermal and hydrological dynamics and changes of growing season in Alaskan terrestrial ecosystems, *Clim. Change*, *107*(3-4), 481–510, doi:10.1007/s10584-010-9988-1.
Thompson, C., J. Beringer, F. S. Chapin, and A. D. McGuire (2004), Structural complexity and land-surface energy exchange along a gradient from arctic tundra to boreal forest, *J. Veg. Sci.*, *15*(3), 397–406.
Wilmking, M., G. P. Juday, V. A. Barber, and H. S. J. Zald (2004), Recent climate warming forces contrasting growth responses of white spruce at treeline in Alaska through temperature thresholds, *Global Change Biol.*, *10*(10), 1724–1736, doi:10.1111/j.1365-2486.2004.00826.x.
Zhang, W., C. Jansson, P. A. Miller, B. Smith, and P. Samuelsson (2014), Biogeophysical feedbacks enhance the Arctic terrestrial carbon sink in regional Earth system dynamics, *Biogeosciences*, *11*(19), 5503–5519, doi:10.5194/bg-11-5503-2014.
Zhu, X., Q. Zhuang, X. Gao, A. Sokolov, and C. A. Schlosser (2013a), Pan-Arctic land-atmospheric fluxes of methane and carbon dioxide in response to climate change over the 21st century, *Environ. Res. Lett.*, *8*(4), 045003, doi:10.1088/1748-9326/8/4/045003.

Zhu, X., Q. Zhuang, Z. Qin, M. Glagolev, and L. Song (2013b), Estimating wetland methane emissions from the northern high latitudes from 1990 to 2009 using artificial neural networks, *Global Biogeochem. Cycles*, *27*, 592–604, doi:10.1002/gbc.20052.

Zhu, X., Q. Zhuang, X. Lu, and L. Song (2014), Spatial scale-dependent land-atmospheric methane exchanges in the northern high latitudes from 1993 to 2004, *Biogeosciences*, *11*(7), 1693–1704, doi:10.5194/bg-11-1693-2014.

Zhuang, Q., V. E. Romanovsky, and A. D. McGuire (2001), Incorporation of a permafrost model into a large-scale ecosystem model: Evaluation of temporal and spatial scaling issues in simulating soil thermal dynamics, *J. Geophys. Res.*, *106*, 33,649–33,670, doi:10.1029/2001JD900151.

Zhuang, Q., et al. (2003), Carbon cycling in extratropical terrestrial ecosystems of the Northern Hemisphere during the 20th century: A modeling analysis of the influences of soil thermal dynamics, *Tellus, Ser. B*, *55*(3), 751–776.

Zhuang, Q., J. M. Melillo, D. W. Kicklighter, R. G. Prinn, A. D. McGuire, P. A. Steudler, B. S. Felzer, and S. Hu (2004), Methane fluxes between terrestrial ecosystems and the atmosphere at northern high latitudes during the past century: A retrospective analysis with a process-based biogeochemistry model, *Global Biogeochem. Cycles*, *18*, GB3010, doi:10.1029/2004GB002239.

Zhuang, Q., J. M. Melillo, M. C. Sarofim, D. W. Kicklighter, A. D. McGuire, B. S. Felzer, A. P. Sokolov, R. G. Prinn, P. A. Steudler, and S. Hu (2006), CO_2 and CH_4 exchanges between land ecosystems and the atmosphere in northern high latitudes over the 21st century, *Geophys. Res. Lett.*, *33*, L17403, doi:10.1029/2006GL026972.

Zhuang, Q., J. He, Y. Lu, L. Ji, J. Xiao, and T. Luo (2010), Carbon dynamics of terrestrial ecosystems on the Tibetan Plateau during the 20th century: An analysis with a process-based biogeochemical model, *Global Ecol. Biogeogr.*, *19*(5), 649–662, doi:10.1111/j.1466-8238.2010.00559.x.

Zhuang, Q., X. Zhu, Y. He, C. Prigent, J. M. Melillo, A. D. McGuire, R. G. Prinn, and D. W. Kicklighter (2015), Influence of changes in wetland inundation extent on net fluxes of carbon dioxide and methane in northern high latitudes from 1993 to 2004, *Environ. Res. Lett.*, *10*(9), 095009.